

# Polyfunctionality of DeNO<sub>x</sub> catalysts in other pollutant abatement

Stefania Albonetti<sup>a,\*</sup>, Joseph Epoupa Mengou<sup>a,b</sup>, Ferruccio Trifirò<sup>a</sup>

<sup>a</sup> Department of Industrial Chemistry and Materials, University of Bologna, Viale Risorgimento 4, 40136 Bologna, Italy

<sup>b</sup> Interuniversity Consortium “Chemistry for the Environment” (INCA), Dorsoduro 2137, 30123 Venezia, Italy

Available online 18 September 2006

## Abstract

The total oxidation of *o*-dichlorobenzene over differently loaded V<sub>2</sub>O<sub>5</sub>/TiO<sub>2</sub>-based catalytic materials was studied. A series of vanadium-supported catalysts have been prepared, by incipient wetness impregnation, on different commercial supports (bare TiO<sub>2</sub>, TiO<sub>2</sub>/WO<sub>3</sub> and TiO<sub>2</sub>/WO<sub>3</sub>/SiO<sub>2</sub>). The prepared materials were characterized by XRD, H<sub>2</sub>-TPR, Raman spectroscopy and surface area measurements. All the catalysts exhibited high oxidation activity and the content of vanadium in the system was demonstrated to be important in controlling the catalyst activity and selectivity. Isolated and well-dispersed vanadium sites resulted beneficial for *o*-DCB conversion. Thus, in spite of the lower ability of SiO<sub>2</sub> to spread metal oxides the higher resistance to sintering of silica-containing materials also at high vanadium content, favors VO<sub>x</sub> dispersion and leads to superior catalytic performance. Nevertheless, the presence of tungsten on the support and of high amount of vanadium also lead to the formation of partial oxidation products. In particular, dichloromaleic anhydride was formed and its production seems to be connected to the distribution of acidic sites.

© 2006 Elsevier B.V. All rights reserved.

**Keywords:** Chlorinated destruction; *o*-dichlorobenzene; SCR catalysts; V<sub>2</sub>O<sub>5</sub>

## 1. Introduction

Stringent environmental regulations are in place in US, Western Europe and Japan, regarding the emissions of polychlorinated dibenzodioxins (PCDDs) and dibenzofurans (PCDFs) [1,2] due to the major health problems associated with the exposure to these compounds [3]. Quaß et al. [4] report the estimates of PCDD/F emissions in Europe for 1985 and 2005 where they indicate that, in spite of being produced by several industrial operations, most of dioxins were produced during municipal solid waste incineration and other combustion processes. Several methods are available today to remove chlorinated organic compounds from waste gas [5], the most used technologies are adsorption on activated carbon [6], wet scrubbing [7] and catalytic total oxidation [8,9]. However, adsorption and absorption techniques only transfer dioxins from the gaseous phase to solid or liquid phase, while the catalytic decomposition causes their real destruction, with the formation of carbon oxides and HCl. Recently, V<sub>2</sub>O<sub>5</sub>/TiO<sub>2</sub>-based catalysts, which are commercially employed for the reduction of NO<sub>x</sub> via NH<sub>3</sub>-SCR, have also been found to be

active for destruction of dioxins, furans and chlorinated organics present in gaseous stream [10–14]. The importance of this kind of catalysts for industrial applications is demonstrated by the number of commercial products present on the market [15,16]. Producers of SCR catalysts and processes claim that modified catalytic systems allow the simultaneous abatement of dioxins and NO<sub>x</sub> in the SCR reactors [17–19]. The optimization of commercial SCR catalysts for the combined dioxins/NO<sub>x</sub> destruction was mainly achieved by increasing the oxidation potential of the catalysts by higher vanadium content. Nevertheless, information provided by commercial producers on these new type of catalysts is very poor and deeper knowledge is required to better understand the relationships between catalytic performance and solid-material properties, which are in turn necessary for further improvement of the catalytic materials and to avoid the possible degradation of catalytic properties during run in commercial plants. In particular, it is known that vanadium-supported material belongs to the most versatile catalysts used for heterogeneous catalytic processes, among them selective oxidation [20,21], and that its catalytic properties are strongly influenced by the structure of the supported vanadium species [22]. Moreover, active species distribution could change during catalyst ageing leading to systems with different properties.

\* Corresponding author. Tel.: +39 051 2093681; fax: +39 051 2093680.

E-mail address: [stalbone@fci.unibo.it](mailto:stalbone@fci.unibo.it) (S. Albonetti).

During our studies in this area, we have investigated the oxidation of 1,2-dichlorobenzene (*o*-DCB) over supported vanadium catalysts. The aim was to elucidate the effect of structural and redox features of differently loaded vanadium/titanium-based catalysts as well as vanadia distribution on catalytic performance. The structural properties and the nature of the vanadium species present on the  $V_2O_5$  catalysts – supported on commercial  $TiO_2$ -based materials (bare  $TiO_2$ ,  $TiO_2/WO_3$  and  $TiO_2/WO_3/SiO_2$ ) – were studied using Raman spectroscopy, X-ray diffraction (XRD) and temperature programmed reduction (TPR). Moreover, with the finding of 2,5-furandione-3,4-dichloro (dichloromaleic anhydride, DCMA) during catalytic oxidation of *o*-dichlorobenzene, never detected before on these type of systems, we evaluated the limits of the destruction of chlorinated waste.

## 2. Experimental

### 2.1. Catalyst preparation

To obtain the supported catalysts, different  $TiO_2$ -anatase commercial powders were used as starting materials: Millennium Chemicals DT51 (bare  $TiO_2$ ), Millennium Chemicals DT52 ( $TiO_2/WO_3 = 90:10$  w/w) and Millennium Chemicals DT58 ( $TiO_2/WO_3/SiO_2 = 81:9:10$  w/w). The vanadium-containing samples were prepared by the method of the incipient wet impregnation procedure which uses an aqueous solution of vanadium oxalate. Vanadium oxalate was synthesized from vanadium pentoxide ( $V_2O_5 > 99.6\%$ , Aldrich) and hot ( $70^\circ C$ ) aqueous solution of oxalic acid ( $>97\%$  Aldrich). The powders obtained were then dried in an oven for 15 h at  $120^\circ C$ , and calcined in air at  $580^\circ C$  for 6 h. Prepared catalysts are reported in Table 1.

### 2.2. Characterization of catalysts

Surface areas were measured by  $N_2$  physisorption apparatus (Sorpty 1750 CE instruments) and single point BET analysis methods, samples were pre-treated under vacuum at  $200^\circ C$ .

Table 1  
Specific surface area, V content, apparent  $VO_x$  surface density and anatase crystallite dimensions for studied catalysts

Catalyst	Specific surface area ( $m^2/g$ )	$V_2O_5$ content (wt.%)	$VO_x$ surface density (V atoms/ $nm^2$ )	Crystallite size $TiO_2$ anatase (nm)
$TiO_2$	76	0	0	20
1.8- $TiO_2$	40	1.8	3.0	30
3- $TiO_2$	36	3.0	5.5	39
5- $TiO_2$	30	5.0	11.0	45
$TiO_2/WO_3$	74	0	0	22
1.8- $TiO_2/WO_3$	61	1.8	2.0	27
3- $TiO_2/WO_3$	44	3.0	4.5	27
5- $TiO_2/WO_3$	36	5.0	9.2	36
$TiO_2/WO_3/SiO_2$	91	0	0	18
1.8- $TiO_2/WO_3/SiO_2$	85	1.8	1.4	20
3- $TiO_2/WO_3/SiO_2$	69	3.0	2.9	22
5- $TiO_2/WO_3/SiO_2$	56	5.0	5.9	27

The reduction behavior of vanadium oxide species was studied by means of TPR using a Termoquest TPDRO instrument. The reducing gas was composed of 5 vol.% of  $H_2$  in Ar. Before reduction the catalysts were heated to  $500^\circ C$  for 1 h in air to achieve the  $V^{5+}$  state.

X-ray diffraction patterns were obtained in the range of  $10$ – $80^\circ$  with a diffractometer Philips PW 1710, using Ni-filtered Cu  $K\alpha$  radiation ( $\lambda = 1.5432 \text{ \AA}$ ). The average crystallite sizes of the synthesized powders were determined from the full-width at half-maximum (FWHM) of the XRD diffraction peaks using the Debye–Scherrer equation.

The Raman spectra were obtained using the 514 nm line of an  $Ar^+$  ion laser, using the Renishaw Raman Spectroscopy System 1000 with Leica DMLM microscope. The laser power at the sample location was 50 mW; the experiments were carried out at ambient conditions.

### 2.3. Catalytic testing

Catalytic experiments were carried out in a fixed bed glass reactor at atmospheric pressure [23]. Each run used approximately 350 mg of catalyst in the form of 30–60 mesh (250–595  $\mu m$ ) particles, mixed with 1120 mg of corundum grains of similar size for better temperature control. The total volumetric flow through the catalyst bed was held constant at 140 ml/min (measured at atmospheric pressure and room temperature), 10 vol.% oxygen, 90 vol.% nitrogen and 1400 ppm of *o*-dichlorobenzene.

Analysis of reactants and products were carried out as follows: the products in the outlet stream were scrubbed in cold acetone maintained at  $-25^\circ C$  by a mixture of dry ice and glycol. The amounts of reagent and products condensed during a reaction period of 15 min at steady state conditions were analyzed with a GC (Perkin-Elmer Autosystem XL) equipped with a PE-17 capillary column (30 m  $\times$  0.25 mm, methylpolysiloxane series) and an electron capture detector (ECD) which uses 1,2-dichloropropane as a standard reference. Additionally, the exit-flow of the reactor trapped in acetone was injected into a GC with a mass selective detector (Hewlett Packard G1800A) to confirm GC data and to verify the formation of non-chlorinated compounds. CO and  $CO_2$  formed were separated on a capillary column Elite Plot Q (30 m  $\times$  0.32 mm), attached to a methanizer and analyzed with a flame ionization detector (FID). Particular care was devoted to determination of the C balance, which was found to always fall between 95 and 105% (calculated as the comparison between converted *o*-dichlorobenzene and the sum of the product yields).

## 3. Results and discussion

### 3.1. Characterization of the catalysts

To investigate the effect of vanadium on the catalyst morphological properties, XRD and surface area measurements have been carried out and reported in Table 1. On this table  $VO_x$  surface density – defined as the number of vanadium atoms per square nanometer of the catalysts – was also reported, since it

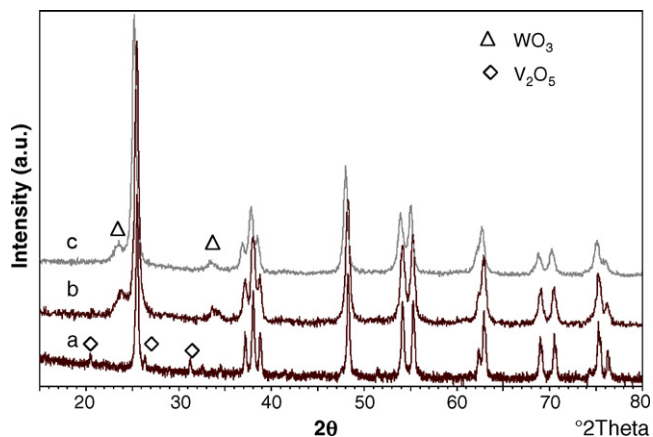


Fig. 1. XRD analysis for different supported catalysts with 5 wt.% of vanadium. (a) 5-TiO<sub>2</sub>, (b) 5-TiO<sub>2</sub>/WO<sub>3</sub> and (c) 5-TiO<sub>2</sub>/WO<sub>3</sub>/SiO<sub>2</sub>.

can provide a convenient parameter to compare materials prepared on supports at different surface area. Obtained data clearly show that a significant loss of surface area and growth in crystallite dimension occur upon V<sub>2</sub>O<sub>5</sub> addition for all studied supports. These phenomena were limited on WO<sub>3</sub>- and SiO<sub>2</sub>-containing samples, thus confirming that the addition of these compounds stabilizes the material against sintering [24,25], retarding the collapse of surface area also for high vanadium presence. These materials, in fact, are generally considered intrinsically unstable due to the catalytic effect of vanadium on the anatase-to-rutile phase transformation [26]. The effect of structure stabilization was mainly observed for silica-containing materials, where the presence of this oxide inhibits the sintering of TiO<sub>2</sub> anatase and preserves surface area. X-ray diffraction analysis of all samples with V<sub>2</sub>O<sub>5</sub> lower than 5 wt.% detected only the lines due to anatase polymorphic form of TiO<sub>2</sub>. This result suggest that, despite the presence of

high amounts of WO<sub>3</sub> and SiO<sub>2</sub> (support DT52, TiO<sub>2</sub>/WO<sub>3</sub> = 90:10 w/w; support DT58, TiO<sub>2</sub>/WO<sub>3</sub>/SiO<sub>2</sub> = 81:9:10 w/w), the materials are well mixed structures, where additives have very good dispersion and are mainly present as amorphous phases. The increase of vanadium content to 5 wt.% leads to the appearance of crystalline V<sub>2</sub>O<sub>5</sub> on 5-TiO<sub>2</sub> sample and of the WO<sub>3</sub> crystallographic phase on the others supported systems (Fig. 1). The segregation of WO<sub>3</sub> indicates a high degree of structure degradation, in fact is generally observed just before the beginning of the anatase to rutile transition [27].

Raman spectra of vanadium supported on titanium under hydrated and dehydrated conditions have been extensively investigated [28,29]. In our Raman studies, taken in air using the pure powder, the absorption bands of anatase at 632, 514, and 390 cm<sup>-1</sup> can be clearly seen, associated with weak peaks at 970–980 and 790–800 cm<sup>-1</sup> (Fig. 2A and B). The higher frequency Raman feature is both associated with W=O and V=O stretching of monomeric wolframyl and vanadyl species that are superimposed on each other, while the band at around 800 cm<sup>-1</sup> consists of both the overlapping contribution of a second-order anatase feature and of the W–O–W stretching mode of structure previously reported. The strong increase in intensity of this last band, on increasing the vanadium content, could be attributed both to increased intensity of the anatase contribution due to higher crystallinity of this phase, and to the growth of crystalline WO<sub>3</sub> already indicated by XRD analysis. Two new Raman bands, at 990 and 694 cm<sup>-1</sup>, attributable to microcrystalline or amorphous V<sub>2</sub>O<sub>5</sub>, appear at higher vanadium loading and with a different distribution due to specific support properties. On silica-containing materials these bands are more pronounced, and present at lower vanadium content, thus indicating a strong effect of SiO<sub>2</sub> presence on vanadium spreading. In effect, these materials revealed not homogeneous distribution of vanadium as well as the presence

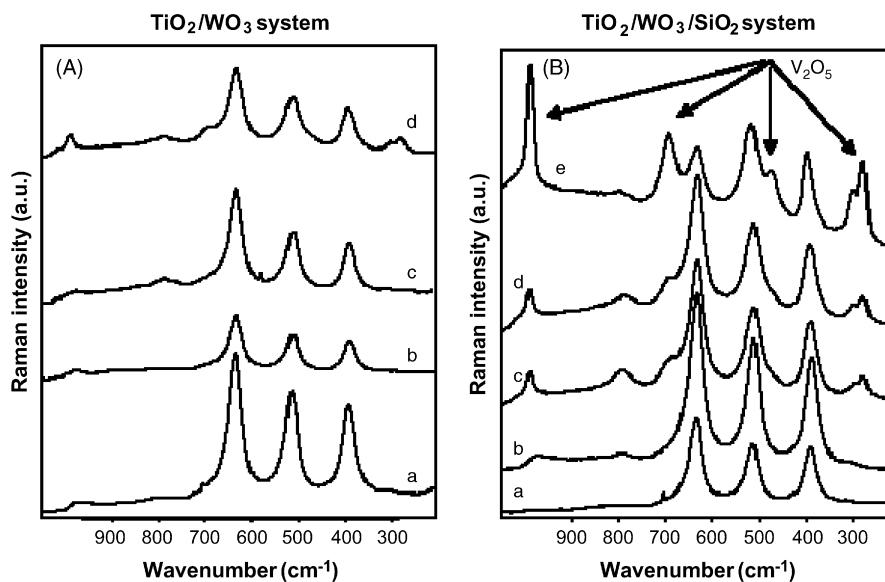


Fig. 2. (A) Raman spectra of TiO<sub>2</sub>/WO<sub>3</sub> based catalysts. (a) V<sub>2</sub>O<sub>5</sub> = 0 wt.%, (b) V<sub>2</sub>O<sub>5</sub> = 1.8 wt.%, (c) V<sub>2</sub>O<sub>5</sub> = 3 wt.% and (d) V<sub>2</sub>O<sub>5</sub> = 5 wt.%. (B) Raman spectra of TiO<sub>2</sub>/WO<sub>3</sub>/SiO<sub>2</sub>-supported vanadium oxide catalysts. (a) V<sub>2</sub>O<sub>5</sub> = 0 wt.%, (b) V<sub>2</sub>O<sub>5</sub> = 1.8 wt.%, (c) V<sub>2</sub>O<sub>5</sub> = 3 wt.%, (d) V<sub>2</sub>O<sub>5</sub> = 5 wt.% and (e) V<sub>2</sub>O<sub>5</sub> microcrystallines in 5-TiO<sub>2</sub>/WO<sub>3</sub>/SiO<sub>2</sub> catalyst.

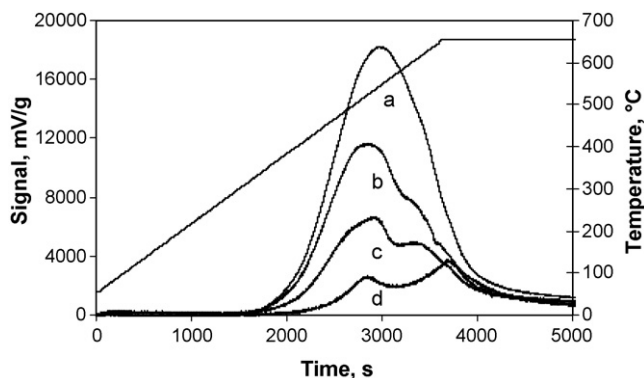


Fig. 3.  $\text{H}_2$ -TPR analysis of  $\text{TiO}_2/\text{WO}_3/\text{SiO}_2$ -supported vanadium oxide catalysts. (a)  $\text{V}_2\text{O}_5 = 5$  wt.%, (b)  $\text{V}_2\text{O}_5 = 3$  wt.%, (c)  $\text{V}_2\text{O}_5 = 1.8$  wt.% and (d)  $\text{V}_2\text{O}_5 = 0$  wt.%.

of micro areas containing bulk  $\text{V}_2\text{O}_5$  starting from sample 3- $\text{TiO}_2/\text{WO}_3/\text{SiO}_2$ , as shown in Fig. 2B, spectra e. This evidence could be explained by hypothesizing that, due to lower capacity of silica to spread vanadium oxide [30], crystalline  $\text{V}_2\text{O}_5$ -like structure are obtained at relatively low vanadium coverage on the surface fraction of the support containing  $\text{SiO}_2$ .

Complementary to the Raman spectroscopic experiments, a clear measure of the variation of the dispersed vanadium phase among supports is provided by the TPR behavior. In Fig. 3 the  $\text{H}_2$ -TPR spectra obtained for  $\text{TiO}_2/\text{WO}_3/\text{SiO}_2$  for increasing vanadium loading are showed as an example. In studied samples, two main reduction peaks were present, with a maximum at 520–545 °C and at about 620 °C, respectively. The low temperature peak can be attributed to the reduction of vanadium highly dispersed and strongly interacting with the support while the high temperature peak is usually ascribed to the reduction of highly polymeric or crystalline vanadia [31]. Nevertheless, as already reported [32], in  $\text{WO}_3$ -containing samples, the exact determination of active species distribution from TPR analysis is rather difficult, due to partial reduction of tungsta in the same region as vanadia. On respect to reported spectra, the peak area of the first peak, mainly due to highly dispersed vanadium, is always higher then the area of the second peak, but with the increase of amount of vanadium to 5 wt.% lead to a significant increase of the higher temperature

peak confirming, as indicated by Raman analysis, the formation of significant quantity of microcrystalline  $\text{V}_2\text{O}_5$ .

### 3.2. Activity measurements

To verify the possibility to increase the oxidation potential of the catalytic systems with the increase of the vanadium loading without production of partial oxidation products, we studied the conversion of *o*-dichlorobenzene (*o*-DCB). The results of *o*-DCB conversion on  $\text{TiO}_2/\text{WO}_3$ -supported catalysts are summarized in Fig. 4a. This figure reports the temperature necessary to have 80% *o*-DCB conversion and  $\text{CO}_x$  selectivity at this temperature, as a function of theoretical  $\text{VO}_x$  density. The reported lines identify  $\text{VO}_x$  surface densities corresponding to theoretical monovanadate ( $2.3 \text{ VO}_x/\text{nm}^2$ ) or polyvanadate ( $7.5 \text{ VO}_x/\text{nm}^2$ ) monolayers [33]. The pure  $\text{TiO}_2/\text{WO}_3$  was found to exhibit some activity for the reaction, mainly due to the  $\text{WO}_3$  presence, but the *o*-dichlorobenzene conversion shows a significant enhancement with the introduction of vanadia. The increase in the vanadia loading changes the system activity. In fact, the *o*-DCB conversion first increases, up to  $\text{V}_2\text{O}_5$   $4.5 \text{ VO}_x/\text{nm}^2$  and then decreases for higher vanadium content suggesting monolayer species to be crucial for catalyst activity.

$\text{CO}$  and  $\text{CO}_2$  were the main products determined. In particular, the selectivity to  $\text{CO}_2$  was in the range 40–60%. Unexpectedly, despite the high selectivity to  $\text{CO}_x$  at high *o*-DCB conversion, as reported in Fig. 4b, significant amount of an incompletely oxidized product, the dichloromaleic anhydride (DCMA) was observed on all catalysts and the formation of this by-product seems to depend on the vanadium loading. In fact, DCMA was formed both at low and high vanadium content but, while on low vanadium content material, it disappeared on increasing DCB conversion, on systems containing a high amount of vanadium, it remained very high. Thus, with all prepared catalysts, *o*-DCB seems to undergo to two parallel reactions: direct oxidation to  $\text{CO}_2$  and  $\text{CO}$  and transformation into an especially stable partial oxidation compound, the dichloromaleic anhydride.

Since silica is commonly used to increase commercial  $\text{DeNO}_x$  catalyst lifetime [24,25], we also investigated the contribution of this compound in the complete oxidation of *o*-DCB. Fig. 5a and b report the effect of different catalyst

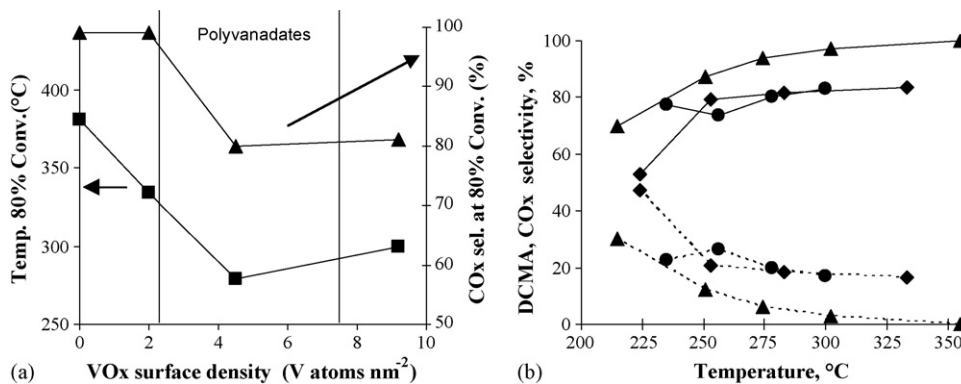


Fig. 4. (a) Temperature of 80% of *o*-DCB conversion (■) and  $\text{CO}_x$  selectivity at 80% of *o*-DCB conversion (▲), as a function of theoretical  $\text{VO}_x$  density for  $\text{TiO}_2/\text{WO}_3$  based catalysts. (b) Product selectivities for samples at different vanadium content.  $\text{V}_2\text{O}_5 = 1.8$  wt.% (▲),  $\text{V}_2\text{O}_5 = 3$  wt.% (●) and  $\text{V}_2\text{O}_5 = 5$  wt.% (◆) ( $\text{CO}_x$  solid line; DCMA dotted line).



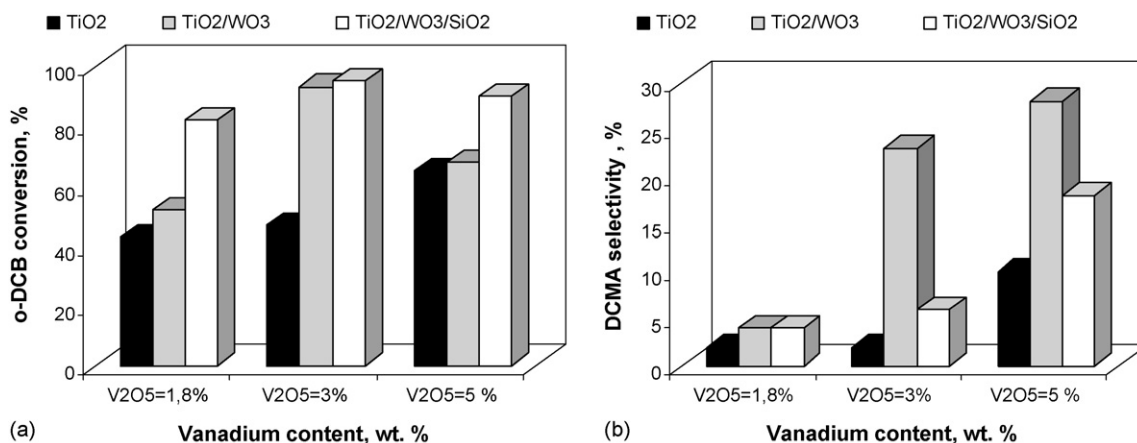


Fig. 5. Effect of different supports on the conversion of *o*-dichlorobenzene (a) and DCMA selectivity (b) over samples at different vanadium content (reaction temperature 300 °C).

composition on *o*-DCB conversion and DCMA selectivity. Both the presence of additives (WO<sub>3</sub> and SiO<sub>2</sub>) and the vanadium content, significantly alter the *o*-DCB oxidation activity of the TiO<sub>2</sub>/V<sub>2</sub>O<sub>5</sub>-based catalysts. In particular, WO<sub>3</sub>-containing samples (TiO<sub>2</sub>/WO<sub>3</sub> and TiO<sub>2</sub>/WO<sub>3</sub>/SiO<sub>2</sub> supports) showed higher activity while the selectivity in DCMA increases with the presence of WO<sub>3</sub> and increasing the vanadium loading.

Trying to correlate the physical–chemical characterization with catalytic results, we can conclude that catalyst activity in *o*-DCB decomposition has the highest value for samples where isolated and polymerized vanadium species dominate, as already indicated for different reactions [34]. Furthermore, it is suggested that the vanadium and tungsten present in bulk-like V<sub>2</sub>O<sub>5</sub> and WO<sub>3</sub> species have only a small catalytic activity, probably because most of the ions are not accessible for the feed. Thus, the lower liability to sintering of silica containing materials, while preserving surface area also at high vanadium content, favors vanadium dispersion and leads to higher catalytic performance. The onset temperatures of the reduction were determined from the TPR curves of all studied materials and reported in Fig. 6 together with the temperature to obtain

80% of *o*-DCB conversion. The fact that the lower onset temperature of reduction was obtained on 3-TiO<sub>2</sub>/WO<sub>3</sub>/SiO<sub>2</sub> sample – which also showed the most interesting catalytic results – seems to indicate that vanadia, bond as highly reducible species on support, is necessary to carry out chlorinated organics degradation.

In addition to the type of vanadium species and to the reducibility of the active phase, the acid–base character of the catalyst could be responsible of the differences of different materials, in particular respect to DCMA formation. Since the acidity of our TiO<sub>2</sub>-based supports, determined by NH<sub>3</sub>-TPD by Vaccari et al. [35] indicated that the relative total acidity of these materials was TiO<sub>2</sub> < TiO<sub>2</sub>/WO<sub>3</sub>/SiO<sub>2</sub> < TiO<sub>2</sub>/WO<sub>3</sub>, different selectivities in DCMA on our materials could be ascribed to the change in acid–basic properties of catalysts due to both the increased vanadium content and the different support acidity. In particular, the presence of surface Brønsted acid sites, due to WO<sub>3</sub> and high vanadium loading [36,37] seems to favors the formation of this product of selective oxidation. On the contrary, Lewis sites, present on titanium oxide and at low vanadium content [38], seem to avoid the DCMA production. Additional studies are ongoing to clarify the mechanism of DCMA formation.

#### 4. Conclusion

These studies demonstrated that the V<sub>2</sub>O<sub>5</sub>-supported titanium-based systems are active for the oxidation of *o*-DCB as well as that VO<sub>x</sub> highly dispersed on the support was the active phase. The vanadium content was found to have a major influence on both the structural stability and catalytic activity of prepared catalysts. In fact, catalysts with a higher vanadium content show a significantly lower surface area. As a consequence, in spite of the lower ability of SiO<sub>2</sub> to spread metal oxides, the higher stability of silica containing materials, while preserving surface area, favors vanadium dispersion and leads to superior catalytic performance.

The formation of dichloromaleic anhydride from *o*-DCB decomposition on these types of catalysts and the catalyst activity could be strongly affected by the acidity of the catalyst;

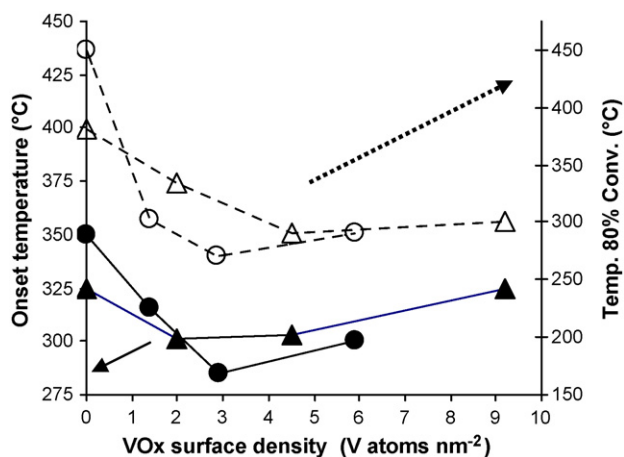


Fig. 6. Comparison between the onset temperature of reduction and the temperature of 80% of *o*-dichlorobenzene conversion for different catalysts. TiO<sub>2</sub>/WO<sub>3</sub> system (●, ○) and TiO<sub>2</sub>/WO<sub>3</sub>/SiO<sub>2</sub> system (▲, △). Onset temperature = filled symbols and *o*-DCB conversion = open symbols.

this indicates that – in order to develop catalysts for complete oxidation of organic molecules – it has to be kept in mind that vanadium oxide is also the main element present in catalysts used for selective oxidation processes and that the stability of possible intermediate products and acidity of the catalyst are key factors in obtaining partial oxidation molecules versus complete decomposition.

## References

- [1] R. Weber, T. Sakai, H. Hagenmeier, *Appl. Catal. B* 20 (1999) 249.
- [2] M. Hiraoka, S. Sakai, T. Sakagawa, Y. Hata, *Organohalogen Compd.* 31 (1997) 446.
- [3] C.W. Davy, *Environ. Int.* 30 (2004) 219.
- [4] U. Quaß, M. Fermann, G. Broker, *Chemosphere* 54 (2004) 1319.
- [5] E. Finocchio, G. Busca, M. Notaro, *Appl. Catal. B* 62 (2005) 12.
- [6] K. Everaert, J. Baeyens, *Waste Manage.* 24 (2004) 37.
- [7] A. Bassetti, M. Bodini, M. Denega, R. Miglio, L. Pistone, W. Tirler, *Organohalogen Compd.* 40 (1999) 445.
- [8] K. Everaert, J. Baeyens, *J. Hazard. Mater.* 109 (2004) 113.
- [9] J. Corella, J.M. Toledo, *Ind. Eng. Chem. Res.* 41 (2002) 1171.
- [10] K.B. Carlsson, *Chemosphere* 25 (1992) 135.
- [11] R. Boos, R. Budin, H. Hartl, M. Stock, F. Wurst, *Chemosphere* 25 (1992) 375.
- [12] M.D. Amiridis, S. Krishnamoorthy, J.A. Rivas, *J. Catal.* 193 (2000) 264.
- [13] R. Weber, M. Plinke, Z. Xu, M. Wilken, *Appl. Catal. B* 31 (2001) 195.
- [14] S. Lomnicki, J. Lichtenberger, Z. Xu, M. Waters, J. Kosman, M. Amiridis, *Appl. Catal. B* 46 (2003) 105.
- [15] <http://www.frauenthal.net/cms/cms.php>.
- [16] <http://www.crienvironmental.com/main.htm>.
- [17] B. Morsbach, P. Odermatt, R. Spahl, BASF AG Report, BASF, Ludwigshafen, Germany, 1992.
- [18] H. Hagenmaier, G. Mittelbach, US Patent 5 512 259 (1996) assigned to Babcock Deutsche Babcock Anlagen AG.
- [19] J.W. Hoj, C.S. Jorgensen, EP Patent 1 524 024 A1 (2004) assigned to Haldor Topsoe A/S.
- [20] B.M. Weckhuysen, D.E. Keller, *Catal. Today* 78 (2003) 25.
- [21] B. Grzybowska-Swierkosz, *Appl. Catal. A* 157 (1997) 263.
- [22] I.E. Wachs, B.M. Weckhuysen, *Appl. Catal. A* 157 (1997) 67.
- [23] S. Albonetti, S. Blasioli, A. Bruno, J. Epoupa Mengou, F. Trifirò, *Appl. Catal. B* 64 (2005) 1.
- [24] L.J. Alemany, L. Lietti, N. Ferlazzo, P. Forzatti, G. Busca, E. Giamello, F. Bregani, *J. Catal.* 155 (1995) 117.
- [25] F. Trifirò, S. Albonetti, S. Blasioli, M. Bugani, S. Angustie, C. Lehaut-Burnouf, E. Roncari, *Environ. Chem. Lett.* 1 (2003) 197.
- [26] G. Olivieri, G. Ramis, G. Busca, V. Sanchez Escribano, *J. Mater. Chem.* 3 (1993) 1239.
- [27] G. Cristallo, E. Roncari, A. Rinaldo, F. Trifirò, *Appl. Catal. A* 209 (2001) 249.
- [28] X. Gao, S.R. Bare, J.L.G. Fierro, I.E. Wachs, *J. Phys. Chem. B* 103 (1999) 618–629.
- [29] L. Lietti, I. Nova, L. Dall'Acqua, E. Giamello, P. Forzatti, *Appl. Catal. B* 35 (2001) 31.
- [30] T. Blasco, J.M. Lopez Nieto, *Appl. Catal. A* 157 (1997) 117.
- [31] D.A. Bulushev, L. Kiwi-Minsker, F. Rainone, A. Renken, *J. Catal.* 205 (2002) 115.
- [32] M.A. Reiche, M. Maciejewski, A. Baiker, *Catal. Today* 56 (2000) 347.
- [33] Khodakov, B. Olthof, A.T. Bell, E. Iglesia, *J. Catal.* 181 (1999) 205.
- [34] B. Grzybowska-Swierkosz, *Top. Catal.* 11/12 (2000) 23.
- [35] S. Albertazzi, C. Barbieri, A. Infantes-Molina, A. Jimenez-Lopez, R. Moreno-Tost, E. Rodriguez-Castellon, A. Vaccari, *Catal. Lett.* 104 (2005) 29.
- [36] G. Ramis, G. Busca, C. Crisitani, L. Lietti, P. Forzatti, F. Bregani, *Langmuir* 8 (1992) 1744.
- [37] I.E. Wachs, B.M. Weckhuysen, *Appl. Catal. A* 157 (1997) 67.
- [38] J. Datka, A.M. Turek, J.-M. Jehng, I.E. Wachs, *J. Catal.* 135 (1992) 186.